AIAA JOURNAL
Vol. 47, No. 3, March 2009

Numerical Study of an Oscillating Airfoil in Transonic Buffeting Flows

Daniella E. Raveh*
Technion—Israel Institute of Technology, 32000 Haifa, Israel

DOI: 10.2514/1.35237

Numerical simulations are conducted to compute the aerodynamic flowfield response that is observed for a NACA0012 airfoil that undergoes prescribed harmonic oscillation at transonic Mach numbers. Large shock oscillations are observed for certain combinations of Mach number and steady mean angle of attack. These are termed as *buffet* in this paper. Prescribing an airfoil oscillation about the buffeting flowfield reveals a nonlinear interaction between the flowfields induced by the buffet and airfoil motion, respectively. At low airfoil-oscillation amplitudes, the time histories of the aerodynamic coefficients exhibit two frequencies, that of the buffet and that of the oscillating airfoil. As the airfoil amplitude increases, the flowfield response at the buffet frequency decreases. Beyond a certain level of airfoil amplitude, lock-in occurs: the flowfield response at the buffet frequency vanishes, and the flow system response predominantly assumes the frequency of the airfoil motion. The airfoil amplitude that will cause lock-in is dependent on the ratio between the frequency of the airfoil oscillation and the buffet frequency. The closer these frequencies are, the smaller the airfoil-oscillation amplitude that will cause lock-in. There is a broad analogy between this flow phenomenon and the flowfield of the von Kármán vortex street found behind a cylinder with the cylinder undergoing a prescribed oscillation. This paper reviews that phenomenon, suggests an aerodynamic gain-phase model for the lock-in region, and suggests a possible relation between this flow mechanism and limit-cycle oscillation.

Nomenclature

c	=	chord length
$\underline{f}$	=	frequency, Hz
f	=	reduced frequency
M	=	Mach number
U_∞	=	velocity, m/s
α	=	angle of attack, deg
α_m	=	mean angle of attack, deg

Introduction

FOR certain combinations of Mach number, airfoil profile, and mean angle of attack, an aerodynamic flow may exhibit large shock oscillations even in the absence of any airfoil motion. This is sometimes termed *buffet* and that is the definition used here. Of course, if the flow is turbulent, there are always small-scale and relatively-small-amplitude fluctuations in the flow. The larger fluid oscillations of interest here are typified by large shock motions and are thought to often, if not always, be a result of shock-induced flow separation. The flow oscillations usually have a characteristic frequency that is called the *buffet frequency* and this is usually expressed as a nondimensional frequency. Given that these large shock oscillations occur, it is of interest to consider the effect on these of forcing the fluid by oscillating the airfoil in a prescribed motion of a certain amplitude and frequency. This airfoil-motion frequency and the buffet frequency and their relationship play a central role in determining the total fluid oscillation that then occurs.

Early encounters of limit-cycle oscillations (LCO) have indicated that the circumstances of these events are sometimes associated with the presence of nonlinear aerodynamic flow phenomena, such as shock-induced separation and shock oscillations (buffet). Cunningham [1] reviewed three incidents of LCO/buffet: LCO driven by leading-edge vortex instability of a B1-A wing of high sweep, LCO driven by shock-induced trailing-edge separation of an F-16 wing, and buffet of F-16 ventral fins. The F-16 LCO, which was encountered during a windup turn of an aircraft carrying two underwing missiles and a new wingtip launcher, led to wind-tunnel testing in which an F-16 wing model was oscillated at different frequencies, amplitudes, mean angles of attack, and Mach numbers [2]. The database of nonlinear aerodynamic pressure distributions collected at these tests was used in an aeroelastic simulation. LCO was simulated at Mach 0.92 and the wing was oscillating at 7.5 Hz at an angle-of-attack amplitude of 0.1 deg and about a mean angle of attack of 5.5–7 deg. As indicated by Cunningham [1], these conditions (namely, the Mach number, frequency, and mean angle of attack) match the conditions of shock-induced separation and shock oscillations. However, Cunningham's studies did not focus on the mechanism of interaction between the oscillating wing and oscillating shock waves, but rather on the development of a LCO-prediction simulation tool.

Edwards et al. [3] presented LCO regions measured at the wind-tunnel test of a business-jet wing in air and heavy gas at a Mach range of 0.8–0.95 at various dynamic pressures and at mean angles of attack of 0.6, 1.6, and 2.1 deg. The authors point to "chimney" regions in which LCO was detected at a constant Mach number of about 0.9 for a range of dynamic pressures. These regions are associated with the first structural bending-mode motion in the heavy-gas experiments and with the first structural torsion-mode motion in the air experiments. The authors indicate that the frequency spectra of the flow showed reduced frequencies that are in the low range of buffet frequencies. Thus, they speculate that in air, an interaction mechanism exists between first torsion and buffet, whereas in heavy gas, the same mechanism exists between the first bending and buffet. The same business-jet wing was analyzed by Edwards [4] using a viscous boundary-layer method coupled with a transonic small-disturbance code. LCO behavior was detected at Mach 0.88, and the flow over the wing was found to be separating and reattaching in the outboard span region. The author concluded that this flow mechanism is responsible for limiting the flutter motion and leads to LCO.

Knipfer and Schewe [5] performed numerical simulations and wind-tunnel tests of a two-degree-of-freedom supercritical two-dimensional section, suspended by springs and dampers, at transonic

Received 21 October 2007; revision received 13 November 2008; accepted for publication 13 November 2008.

*Senior Lecturer, Faculty of Aerospace Engineering. Member AIAA.

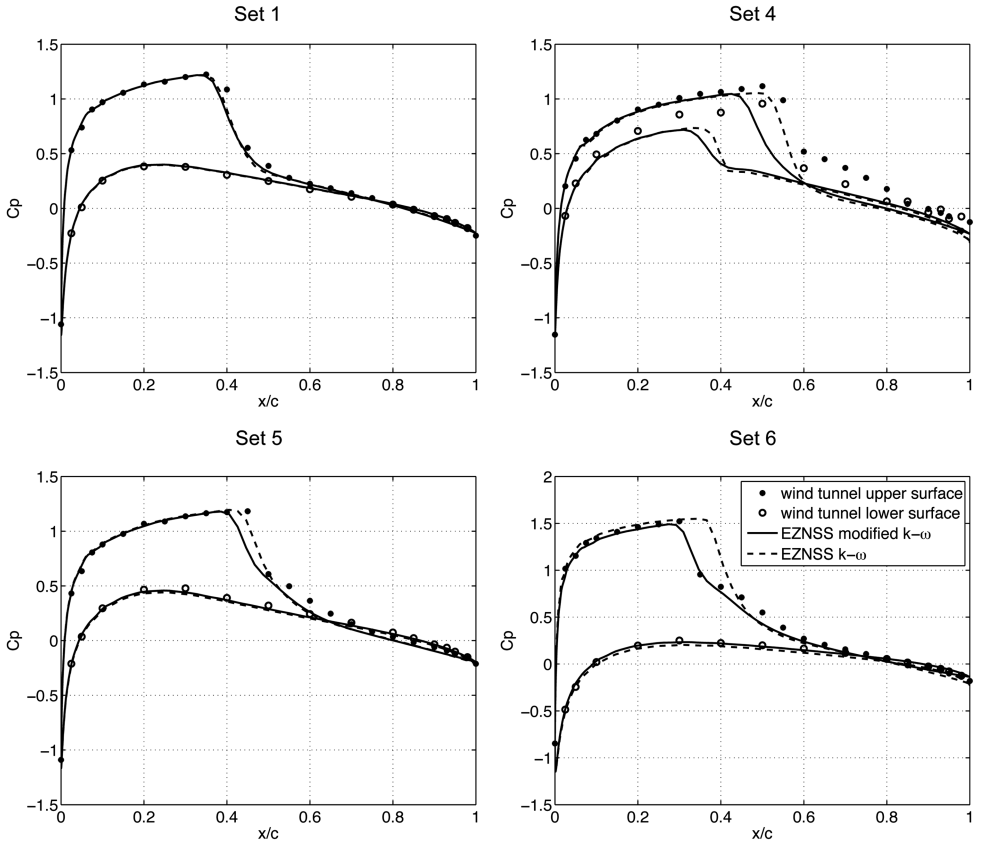

Fig. 1 Comparison of EZNSS-computed and McDevitt and Okuno's [10] wind-tunnel-test pressure-coefficient distribution.

flows. The Navier–Stokes simulation, which used the Baldwin–Lomax turbulence model, was able to predict the flutter points. However, as the authors indicate, this turbulence model was inadequate for assessing boundary-layer interaction and buffet phenomena. The flutter points of the experiment exhibited limit-cycle amplitudes, some of which occurred at Mach numbers below the buffet limit. Thus, the authors concluded that LCO is not caused by buffet, but rather emerges from classical flutter. Dowell and Tang [6], and Thomas et al. [7] studied the role of nonlinear aerodynamics in LCO. They suggested that large shock translations and flow separation are the main effectors of aerodynamic nonlinearity leading to LCO. However, the flows they studied were all inherently stable and did not buffet.

The current study focuses on the relationship between buffet and airfoil motions and the aerodynamic forces that develop when an airfoil is oscillated in buffeting flows. This is done by simulating responses of the flowfield for a NACA0012 airfoil with prescribed harmonic excitation at flight conditions that exhibit strong shock oscillations. It is hoped that these time simulations can provide insight to help answer questions regarding the nature of nonlinear responses, such as the following: How nonlinear is the transonic flowfield response of an oscillating wing? Is it nonlinear simply due to the presence of the shock wave, or is it the shock travel that causes the response to be nonlinear? How do the airfoil oscillations interact with the traveling shock? How is the response dependent on parameters such as Mach number, mean flow angle of attack, oscillation frequency, angle of attack, and possibly other parameters? Finally, can wing buffet be a source of LCO? That is, does the oscillating shock wave excite the wing? Or is wing buffet a restraining factor that causes flutter to become LCO?

Computational Fluid Dynamics Simulation

The unsteady-flow simulations of this study were performed using the Elastic Zonal Navier–Stokes Simulation (EZNSS) computational fluid dynamics (CFD) code [8]. EZNSS is a finite difference code employing several optional flow solver algorithms and turbulence models. The accuracy of the unsteady buffet simulation is dependent to a great extent on the numerical scheme, the accuracy and suitability of the turbulence model used, and the choice of run parameters, such as grid and time step. The algorithm used in this study is the Steger–Warming algorithm. This algorithm was chosen as it involves minimal numerical dissipation, which could possibly quench the studied phenomena. Barakos and Drikakis [9] assessed the adequacy of several turbulence models for transonic buffet problems. Using the same wind-tunnel test that is used for validation in the current study (McDevitt and Okuno [10]) they compared various turbulent closures, including the algebraic Baldwin–Lomax model, the one-equation Spalart–Allmaras model, linear and nonlinear k-ε models, and a nonlinear k-ω model version with constant and functional c_μ coefficients. Barakos and Drikakis [9] concluded that nonlinear two-equation models in conjunction with a

Table 1 Data sets of McDevitt and Okuno's wind-tunnel test used for validation

Set	M_N	α_N, deg	M_∞	α, deg
1	0.75	2	0.751	1.99
4	0.8	1	0.793	1.00
5	0.775	2	0.775	2.05
6	0.725	4	0.726	3.91

Table 2 Buffet onset frequencies at McDevitt and Okuno's [10] wind-tunnel test ($\bar{f}$) and from simulation ($\bar{f}_{\text{sim}}$)

Set	M_∞	α, deg	$\bar{f}$	$\bar{f}_{\text{sim}}$
1	0.75	4	0.47	0.45
4	0.80	4	0.38	0.43
5	0.77	4	0.44	0.51
6	0.72	6	0.55	0.59

functional c_μ coefficient provide adequate results for transonic buffet flows. Following the findings of Barakos and Drikakis, the steady pressure-coefficient distribution at the four wind-tunnel-test cases reported by McDevitt and Okuno [10] was computed by EZNSS using two turbulence models: the k-ω model and the modified k-ω model [11]. The latter is a recent modification to the k-ω model that is reported by its developer to be suitable for a wider range of mildly separated flows. Because there is little information available on the suitability of various turbulence models for unsteady problems, the strategy in choosing an adequate model was to first check its suitability in the steady case (at an angle of attack at which there is no buffet) and to then use the best model for the unsteady buffeting case, comparing the computed buffet parameters with those from wind-tunnel tests. Results are reported in the Test Case section. Following validation, further analyses were performed using the modified k-ω model.

The computational domain is covered by a C-type grid extending approximately 18 chords away from the profile. There are 401 grid points in the chordwise direction, along the profile and its wake, and 75 grid points in the direction perpendicular to the surface. The distance of the first grid point off of the wall in the perpendicular direction is 1×10^{-5} chords. Adequacy of the computational grid to the current analysis was established by studying grids of various dimensions. To verify that the grid extension to the far field is adequate and that the phenomena observed are not a result of inward flow reflections from the computational boundaries, some of the analyses were repeated on a grid extending only 10 chords out. The flowfield was found to be the same as for the 18-chords-out grid, and the rest of the analyses were computed with the 18-chords-out grid. For comparison, Barakos and Drikakis [9] studied the same test case with a similar-sized grid of 361 by 90 points, extending 7 chords away from the profile.

Test Case

The test case studied is that of a NACA0012 section oscillating in heave and pitch motions. This test case was chosen because there are ample wind-tunnel-test data in the literature to support code validation. The issue of code validation is crucial in this study, because the flows simulated are highly viscous and involve shock/boundary-layer interaction. It was found during this study that some of the commonly used CFD algorithms and turbulence models involve a large amount of numerical dissipation that eliminates, or significantly alters, the flow phenomena studied. Thus, it was important to validate the chosen algorithm and turbulence model using both static and dynamic wind-tunnel-test data.

Validation of CFD results was performed based on wind-tunnel tests by McDevitt and Okuno [10] and those by Landon [12]. McDevitt and Okuno [10] performed static and dynamic pressure measurements on a NACA0012 airfoil at Mach numbers of 0.7 to 0.8, at Reynolds numbers of 1×10^6 to 14×10^6, and for a range of angles of attack that include the onset of buffet. In these wind-tunnel tests, sidewall boundary-layer removal was used to minimize the sidewall interference effects, such that the resulting streamlines would closely match those of free air. As a result, the measurements of McDevitt and Okuno are particularly favorable for CFD code validation.

Static-pressure data were measured at six combinations of angles of attack and Mach numbers. Following the recommendation of the authors, the test data at Reynolds number of approximately 10×10^6 are used for code evaluation. Table 1 presents the four data sets that were used for validation in this study. The nominal angle of attack and Mach number values, denoted by the subscript N, are the values for which the wind-tunnel walls were tuned. The actual test values are denoted by M_∞ and α. Figure 1 presents pressure-coefficient distribution on the upper and lower surfaces of the airfoil for the four validation data sets. The stars and circles represent measured pressure coefficients on the upper and lower surfaces, respectively, and the full lines represent values computed in an EZNSS simulation with the k-ω and modified k-ω turbulence models. Figure 1 shows that the modified k-ω model closely captures the measured pressure-coefficient distribution for all but set 4. Further unsteady analyses were therefore performed using the modified k-ω turbulence model.

McDevitt and Okuno [10] performed an angle-of-attack sweep about the four nominal sets 1, 4, 5, and 6 to capture the buffet-onset conditions. Table 2 presents the Mach number and angle of attack at which buffet phenomena appeared and the buffet's reduced frequency. The test reduced frequency $\bar{f}$ is defined as

$$\bar{f} = \frac{2\pi f c}{U_\infty} \tag{1}$$

Buffet conditions were simulated in EZNSS runs by computing the unsteady responses to a step angle of attack of amplitudes corresponding to the test buffet angles of attack (as defined in Table 2). The analyses were started from initial steady-state flow conditions corresponding to a 0 deg angle of attack at the Table 2 Mach numbers. All tests and simulations were performed at Reynolds number of 10×10^6. Table 2 presents the simulated buffet reduced frequencies $\bar{f}_{\text{sim}}$ evaluated from EZNSS simulations according to Eq. (1) using the CFD reference chord length of 1. Table 2 results show that the EZNSS simulations capture the reduced frequency of the buffet phenomena relatively accurately, but they are less accurate at the higher Mach numbers. This is also consistent with the static-pressure-coefficient distribution results that are more accurate at the lower Mach numbers. Therefore, it was decided that further unsteady simulations will be performed at Mach 0.72.

Another important factor for the accuracy of the simulation is the simulation time step. The effect of the simulation time step on the computed responses is discussed in Appendix A.

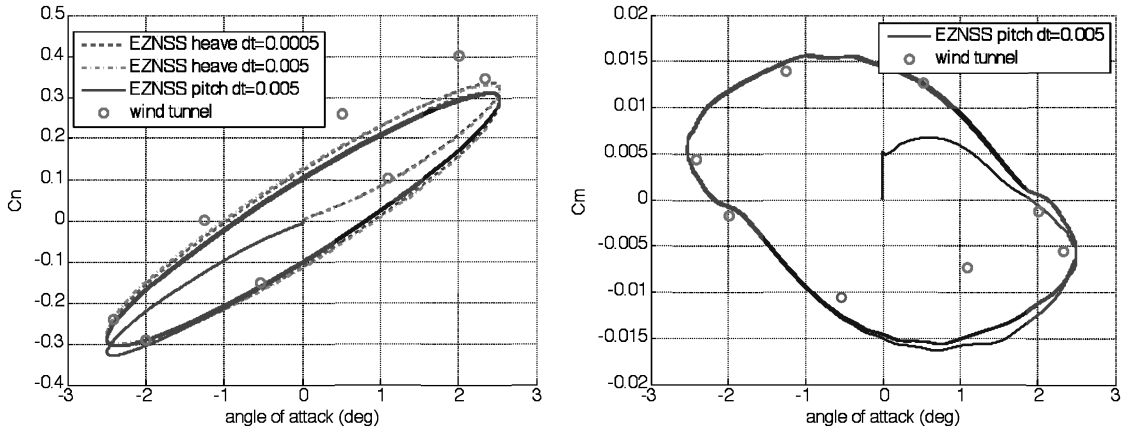

a) b)

Fig. 2 Angle of attack vs a) normal-force coefficient and b) moment coefficient about the quarter-chord in response to sinusoidal excitation at Mach 0.755, $\alpha = 2.51$ deg, and $\alpha_m = 0.016$ deg, computed by EZNSS and recorded at Landon's [12] wind-tunnel test.

Figure 2 presents validation of prescribed airfoil harmonic simulations using wind-tunnel experiments of an oscillating NACA0012 airfoil by Landon [12]. Figure 2 presents the normal-force coefficient and moment coefficient versus angle of attack in response to prescribed sinusoidal pitching and heaving motions, with an amplitude of 2.51 deg about a mean angle of attack of 0.016 deg at a reduced frequency of 0.1628 [based on Eq. (1)] and at a Mach number of 0.755. EZNSS simulations were performed using time steps of 0.005 and 0.0005. All numerical simulations yielded similar results, which reasonably match those of the wind-tunnel tests. The trend of the correlation between the simulations and wind-tunnel-test results is similar to those of simulations performed using other CFD codes, as presented in Fig. 14 of [13].

Responses to Sinusoidal Heave Excitations

Following code validation, responses to prescribed sinusoidal heave motions at various conditions were simulated. Figure 3 presents lift- and moment-coefficient responses to heave excitations of various frequencies for a heave velocity that corresponds to an angle-of-attack amplitude of 6 deg. The responses were computed at Mach 0.72, a Reynolds number of 10×10^6, and about a 0 deg mean angle of attack. All CFD simulations were performed using a computational time step of 0.001. At these flow conditions, there is no buffet at the mean angle of attack. As the oscillatory angle of attack is increased in the course of the cycle, a shock wave builds up and oscillates. The cycle's maximum angle of attack was chosen such

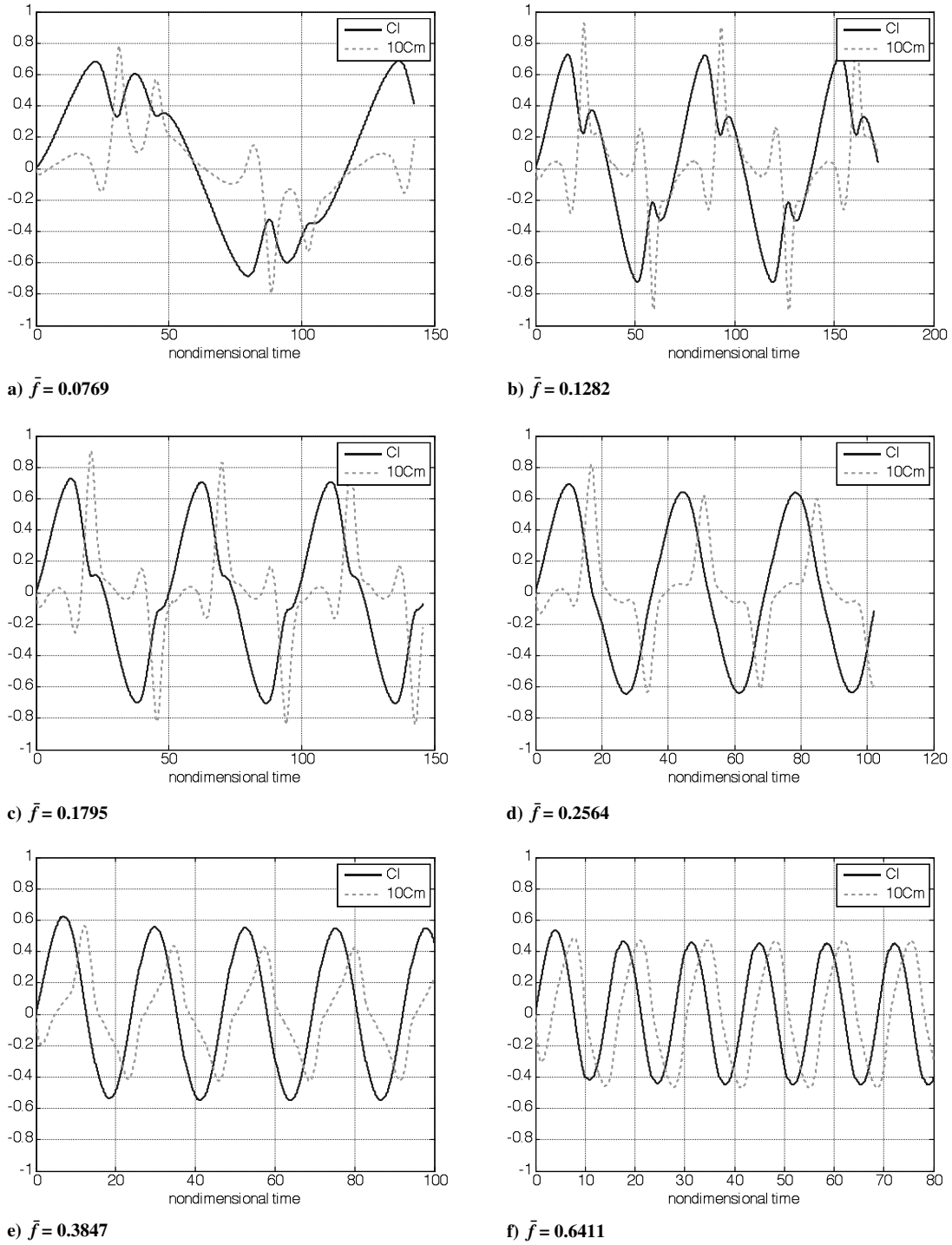

a) $\bar{f} = 0.0769$ b) $\bar{f} = 0.1282$

c) $\bar{f} = 0.1795$ d) $\bar{f} = 0.2564$

e) $\bar{f} = 0.3847$ f) $\bar{f} = 0.6411$

Fig. 3 Lift coefficient and 10 times the moment coefficient about the quarter-chord vs time in response to sinusoidal excitations at various frequencies; $\alpha = 6\,\text{deg}$, $\alpha_m = 0\,\text{deg}$, Mach 0.72, and $Re = 10 \times 10^6$.

that buffet was observed in wind-tunnel tests at a steady angle of attack of the same magnitude and was simulated successfully by EZNSS (as discussed in the Test Case section).

Figure 3 presents the effect of the oscillating shock wave on the aerodynamic lift and moment at different frequencies. At excitation frequencies that are significantly lower than the buffet frequency (e.g., Figs. 3a and 3b), fluctuations of the lift and moment coefficients are observed, which correspond to shock forward and backward travel. The oscillating shock appears as a higher-frequency response on top of the heave-oscillation response, but only at those parts of the cycle at which the angle of attack is above a certain value (also see Figs. 4a–4c). At low excitation frequencies, the oscillating shock quenches the aerodynamic coefficient values. At the higher excitation frequencies above the buffet frequency (Fig. 3f), the shock does not seem to affect the response significantly. This is also seen from Fig. 4, which presents the lift coefficient vs angle of attack. At an excitation frequency above the buffet frequency (Fig. 4f), the response seems to display only a single harmonic.

Because the buffet appears only in certain segments of the cycle and not throughout, its frequency cannot readily be detected by Fourier analysis. Measured from the peak-to-peak time at the lowest excitation frequency (Fig. 3a), this frequency $\bar{f} = 0.59$, which is the same buffet frequency that was measured in static analysis (Table 2).

The simulations of Figs. 3 and 4 suggest the nature of interaction between the airfoil oscillation and buffet. However, the simulated

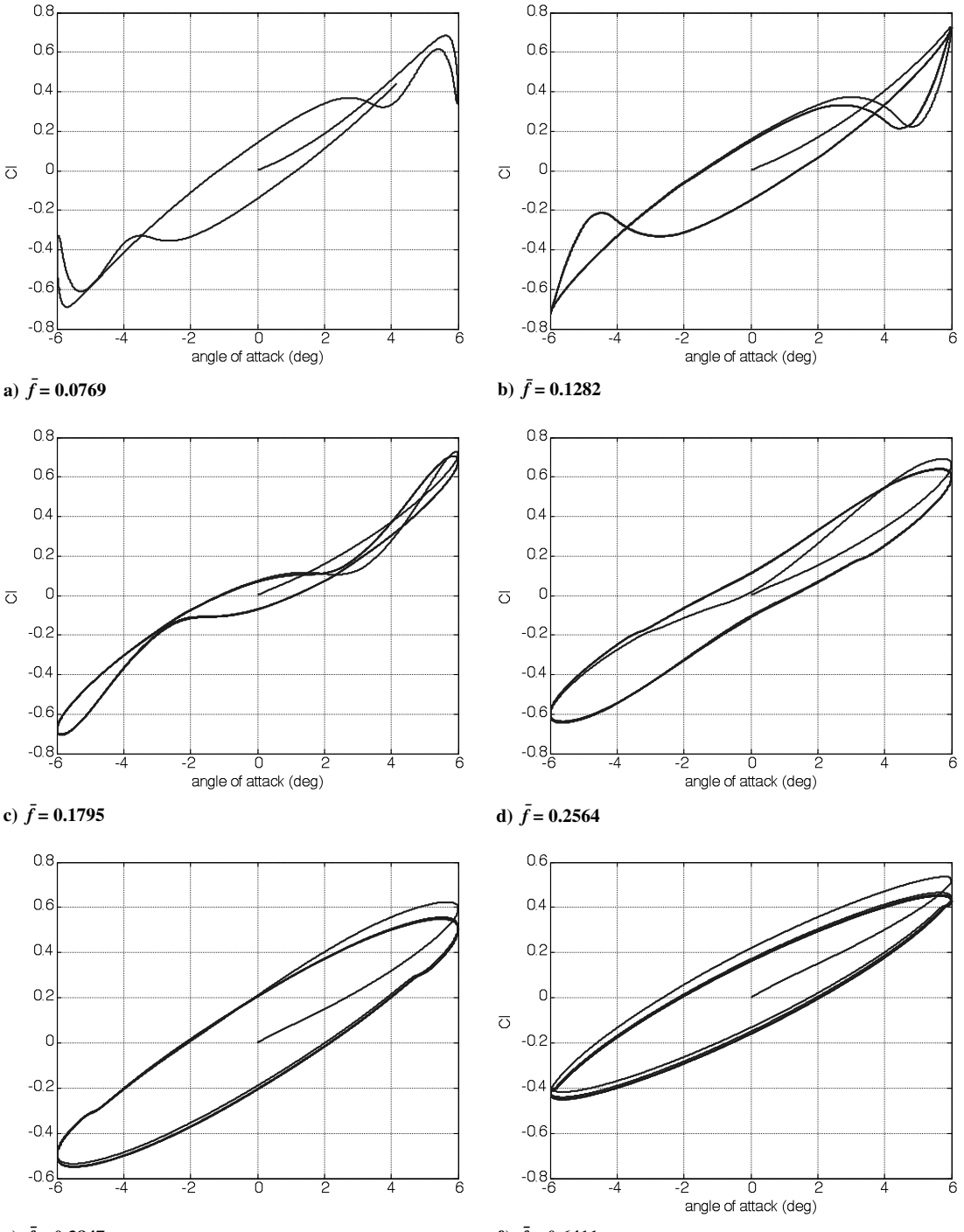

a) $\bar{f} = 0.0769$ **b)** $\bar{f} = 0.1282$

c) $\bar{f} = 0.1795$ **d)** $\bar{f} = 0.2564$

e) $\bar{f} = 0.3847$ **f)** $\bar{f} = 0.6411$

Fig. 4 Lift coefficient vs angle of attack in response to sinusoidal excitations at various frequencies; $\alpha = 6\,\text{deg}$, $\alpha_m = 0\,\text{deg}$, Mach 0.72, and $Re = 10 \times 10^6$.

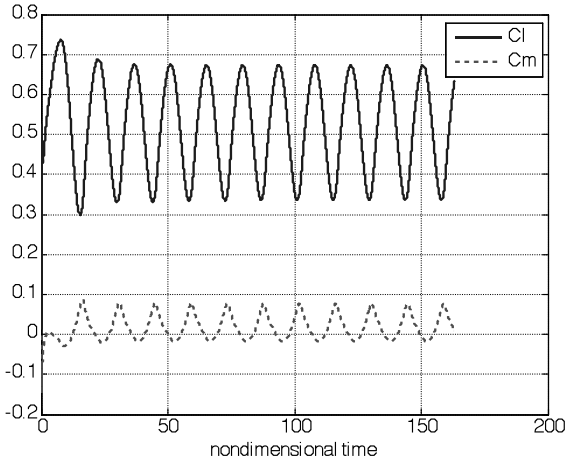

Fig. 5 Lift and moment coefficients in a buffeting flow; $\alpha_m = 6$ deg, Mach 0.72, and $Re = 10 \times 10^6$.

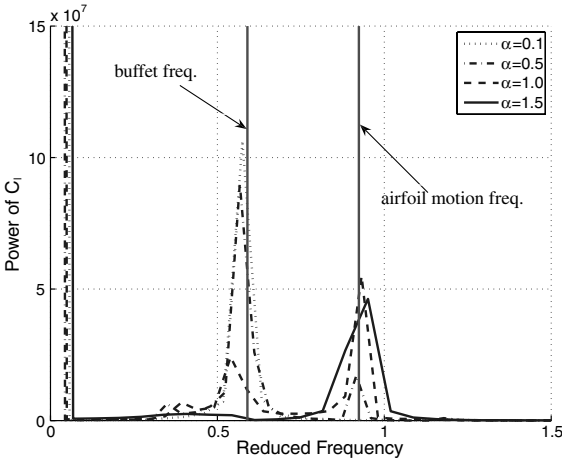

Fig. 6 Frequency content of the lift coefficient in response to forced heave excitation of $\bar{f} = 0.92$; $\alpha = 1.0$ deg, $\alpha_m = 6$ deg, Mach 0.72, and $Re = 10 \times 10^6$.

conditions, those of ± 6 deg about a 0 deg mean angle of attack, are not typical of flight aeroelastic phenomena. To study the interaction of elastic oscillation and buffet, which develop in realistic flight conditions, the heave forced-oscillation simulation was repeated, exciting the airfoil at various frequencies and amplitudes, about a 6 deg mean angle of attack, at Mach 0.72, and at a Reynolds number of 10×10^6. The mean angle of attack of 6 deg is typical of windup turns, and the forced-oscillation amplitudes ranging between 0.1 and 1.5 deg are typical of elastic motions at LCO.

Figure 5 presents the time history of the aerodynamic coefficients in response to a *steady* angle of attack of 6 deg. The oscillations are due to buffet, with a buffet reduced frequency of $\bar{f} = 0.59$. The mean lift coefficient equals 0.5, and the moment coefficient, which is computed about the quarter-chord, changes its sign as the shock crosses in front of and behind the quarter-chord point. The airfoil was oscillated in heave for various frequencies, ranging from below to above the buffet frequency, with heave velocities that correspond to angle-of-attack amplitudes of 0.1, 0.5, 1, and 1.5 deg.

A sample response is shown in Fig. 6 that presents the frequency content of the lift response to prescribed airfoil-motion excitation at a reduced frequency of $\bar{f} = 0.92$, which is above the buffet frequency.

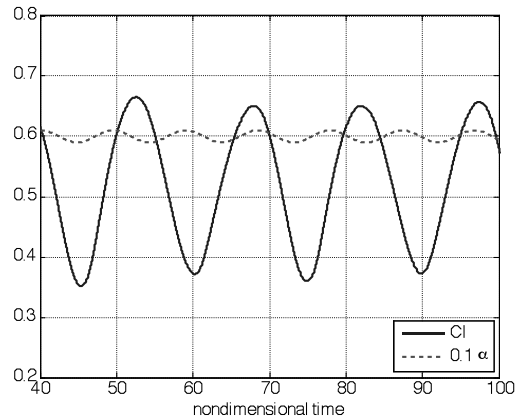

a) $\alpha = 0.1$ deg

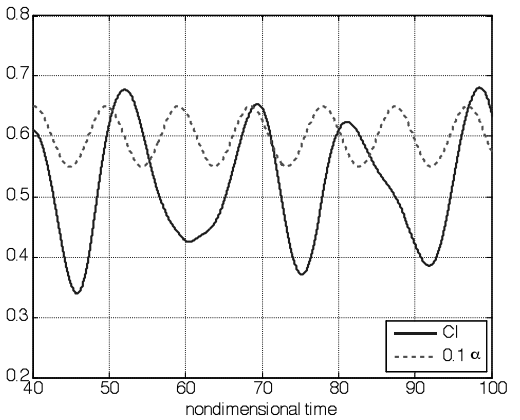

b) $\alpha = 0.5$ deg

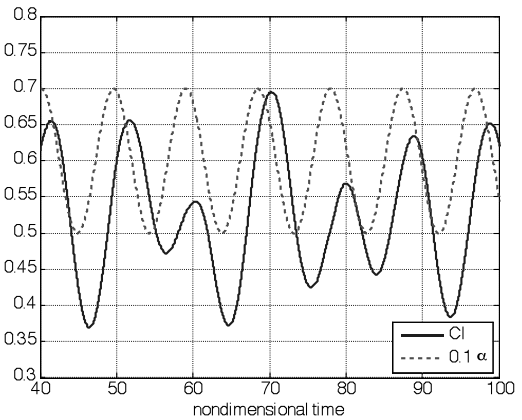

c) $\alpha = 1.0$ deg

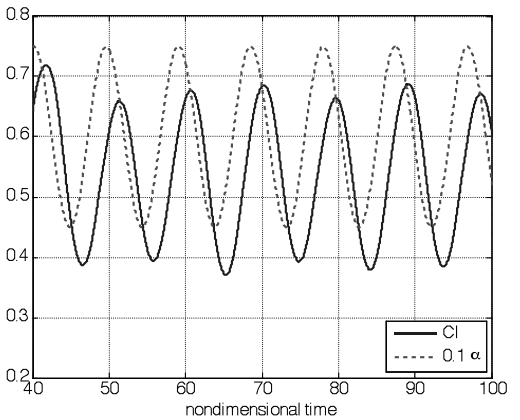

d) $\alpha = 1.5$ deg

Fig. 7 Time histories of the lift coefficient and angle of attack in response to excitations of various amplitudes; $\bar{f} = 0.92$, $\alpha_m = 6$ deg, Mach 0.72, and $Re = 10 \times 10^6$.

For small amplitudes of airfoil-motion excitation, the flow system response exhibits two distinct frequencies: that of the buffet and that of the excitation. At the lowest amplitudes of excitation ($\alpha = 0.1$ deg, dotted line), most of the response power is in the buffet frequency. As the amplitude of excitation increases ($\alpha = 1$ deg, dashed line), there is more power in the excitation frequency and less power in the buffet frequency. As the amplitude of excitation is further increased ($\alpha = 1.5$ deg, full line), the buffet vanishes and the system's response is in the airfoil-motion-excitation frequency only. Figure 7 presents the time histories of the lift responses that were used to compute the frequency content of Fig. 6. The time history of the airfoil-motion input is also plotted, so that it is easy to observe the frequency of the response in relation to the frequency of the excitation. It is seen that at the lower amplitude of airfoil-motion excitation, the buffet frequency dominates the flow (Fig. 7a). As the amplitude is increased, both frequencies appear, and the response is beating (Figs. 7b and 7c). As the amplitude is further increased, the response assumes the frequency of airfoil-motion excitation (Fig. 7d).

Simulations for prescribed airfoil-motion excitations were repeated at various frequencies. Figure 8 presents the frequency content of some of these responses. They all exhibit the same phenomenon of the buffet frequency fading out with increased

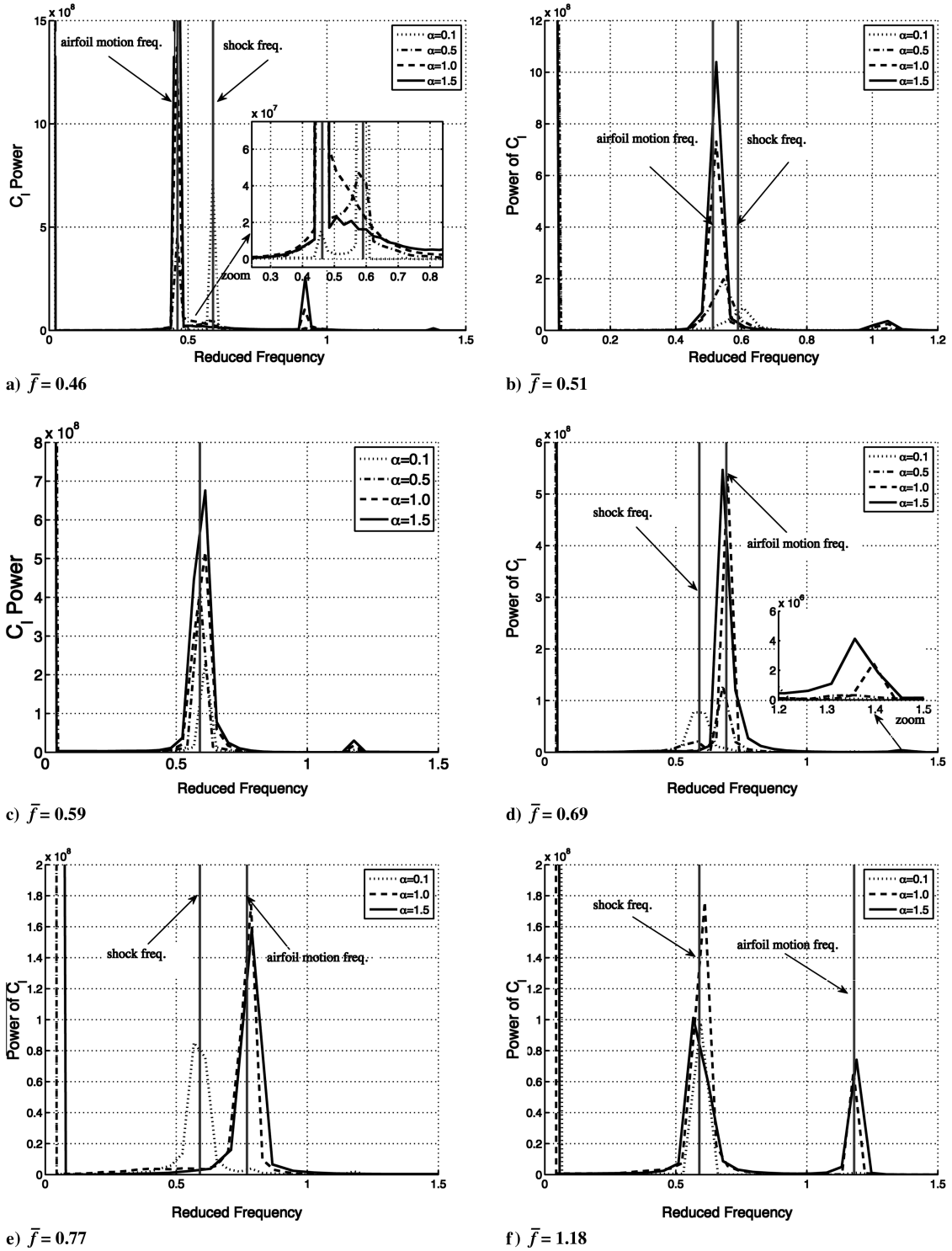

Fig. 8 Frequency content of lift-coefficient response to airfoil-motion excitations of various amplitudes and frequencies; $\alpha_m = 6$ deg, Mach 0.72, and $Re = 10 \times 10^6$.

airfoil-motion amplitude. Figure 8 shows that the closer the airfoil-motion frequency to the buffet frequency, the smaller the amplitude that will eliminate the buffet. This is also seen in Fig. 9, which presents time histories of the lift responses to airfoil-motion excitations of frequencies ranging from below to above the buffet frequency, all corresponding to an amplitude of airfoil motion of 1 deg. At frequencies significantly lower than the buffet (Figs. 9a and 9b) and significantly higher than the buffet (Figs. 9h–9j), the response is a combination of the airfoil-motion and buffet frequencies. At frequencies close to the buffet frequency (Figs. 9d–9g), this amplitude of airfoil motion is sufficient to suppress the buffet, and the system response is solely in the airfoil-motion frequency. Based on this observation, Fig. 10 defines regions of combinations of frequencies and amplitudes of airfoil-motion

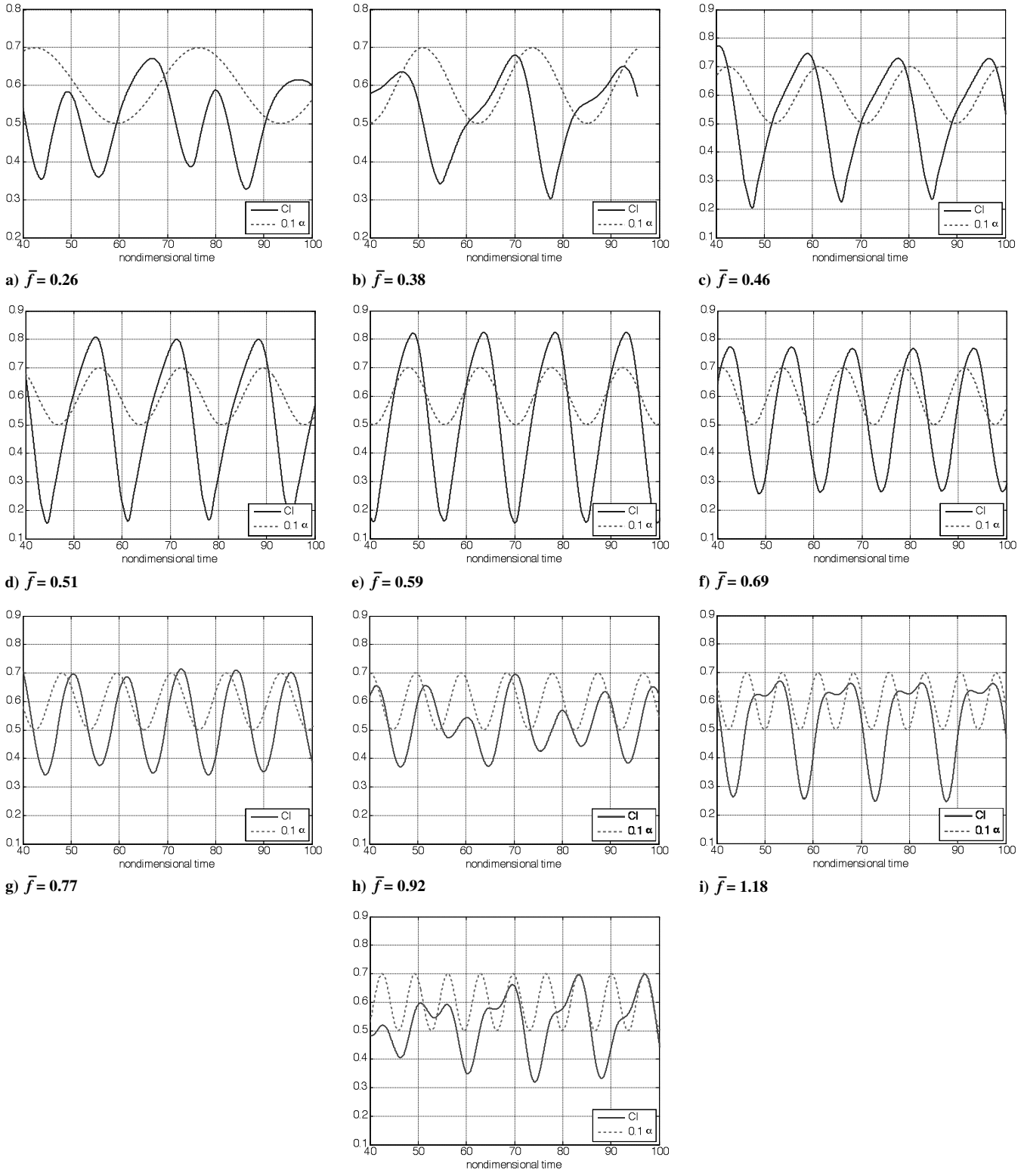

a) $\bar{f} = 0.26$ **b)** $\bar{f} = 0.38$ **c)** $\bar{f} = 0.46$

d) $\bar{f} = 0.51$ **e)** $\bar{f} = 0.59$ **f)** $\bar{f} = 0.69$

g) $\bar{f} = 0.77$ **h)** $\bar{f} = 0.92$ **i)** $\bar{f} = 1.18$

j) $\bar{f} = 1.28$

Fig. 9 Time histories of the lift coefficient and angle of attack in response to excitations of various frequencies; $\alpha = 1.0$ deg, $\alpha_m = 6$ deg, Mach 0.72, and $Re = 10 \times 10^6$.

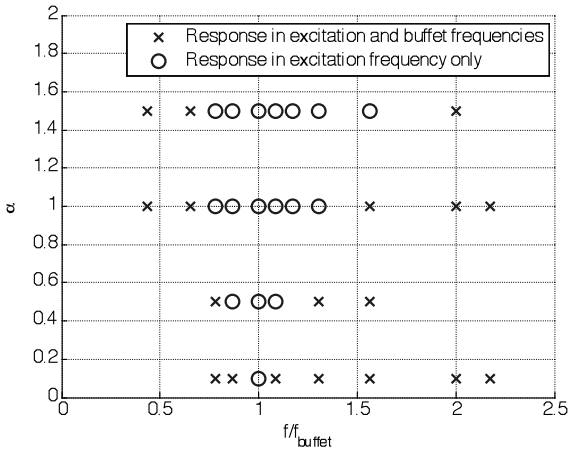

Fig. 10 Combinations of excitation frequencies and angles of attack leading to responses in both the excitation and buffet frequencies and in the excitation frequency only; $\alpha_m = 6$ deg, Mach 0.72, and $Re = 10 \times 10^6$.

excitations for which the system response is in the airfoil-motion-excitation frequency only and regions in which the response involves both the buffet and airfoil-motion frequencies. This phenomenon resembles the lock-in phenomenon found for oscillating cylinders in shedding flows of low Reynolds numbers [14,15] and, recently, for the case of a plunging airfoil at a low Reynolds number of 20,000 [16]. These reported lock-in phenomena, however, are all at low Reynolds numbers and at higher frequencies. To the best of the author's knowledge, lock-in was never reported in transonic high-Reynolds-number flows at frequencies that are within the range of typical aircraft structural response frequencies.

Another thing to note from Fig. 8 is that the responses involve higher harmonics, the first of which is at about double the airfoil-motion frequency. However, Fig. 8 shows that as the frequency of airfoil-motion excitation grows larger, this higher harmonic has less power in it. For modeling purposes, this may indicate that at the high frequencies, the higher harmonics may be neglected.

Focusing on the cases in which the buffet is suppressed and the system responds in the airfoil-motion-excitation frequency only (Figs. 9c–9g), we note the following:

1) The lift responses are symmetric about a lift-coefficient value of 0.5, which is the mean lift-coefficient value of the steady buffeting flow (see Fig. 5).

2) At airfoil-motion-excitation frequencies below the buffet (Figs. 9c and 9d), the lift response is leading the angle-of-attack motion, whereas at frequencies above the buffet (Figs. 9f and 9g), the lift is lagging the angle-of-attack motion. Close to the buffet frequency, the lift response and angle of attack are in phase.

3) At the lower frequencies (Figs. 9c and 9d), the lift response is not harmonic. The lift rises gradually with increasing angle of attack and then drops instantaneously. This phenomenon may correspond to the high-frequency content shown in Fourier analysis (Figs. 8a–8d). At airfoil-motion frequencies above the buffet, the lift response is harmonic, consisting of a single harmonic.

Based on these observations, a simple gain and phase model can be extracted, as shown in Fig. 11. This model was constructed from the time histories of responses to $\alpha = 1.5$ deg, assuming that the responses for this value of excitation include only one harmonic at the airfoil-motion-excitation frequency. The steady angle of attack was deduced from the excitation amplitude, and the mean values of the aerodynamic coefficients at the steady buffeting flow (Fig. 5) were deduced from the responses. This is not valid when the frequency of excitation equals the buffet frequency. Nevertheless, the model of Fig. 11 presents a simple behavior of the aerodynamic coefficients in the lock-in region. The lift-curve slope peaks near the buffet frequency and its phase changes signs. The moment-coefficient-curve slope reduces with frequency and its phase is 180 deg, with the excitation at the buffet frequency. Further study involving an aeroelastic model is required to determine whether this has an effect on initiating LCO-type responses.

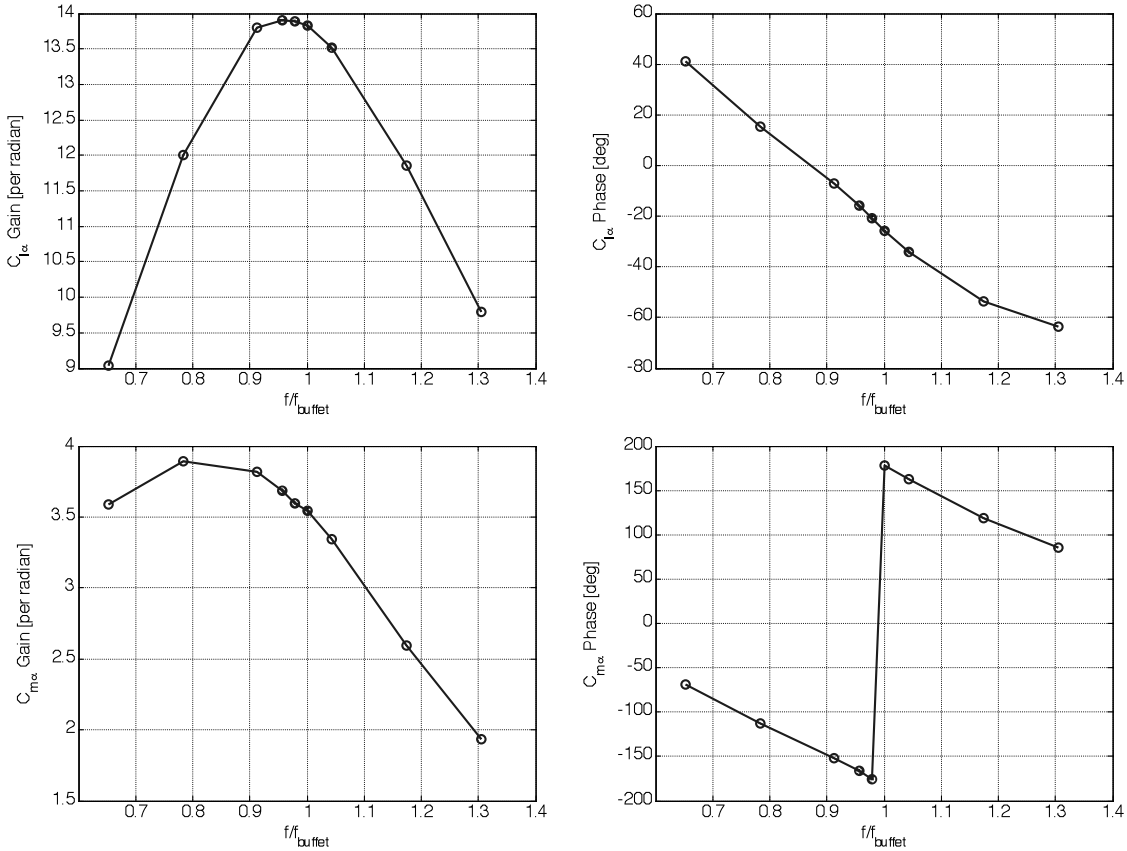

Fig. 11 Lift- and moment-curve slopes vs frequency ratio; $\alpha = 1.5$ deg, $\alpha_m = 6$ deg, Mach 0.72, and $Re = 10 \times 10^6$.

The buffet-airfoil-oscillation interaction may be related to the LCO phenomenon, providing both the excitation force and the restraining mechanisms, as follows: At flight speeds close to flutter, at which an elastic mode is becoming only lightly damped, the unsteady buffet may serve as an external excitation force, initiating elastic modal oscillations of increasing amplitudes. As the elastic amplitudes increase, lock-in occurs, and the exciting force is decreased. Thus, LCO is maintained. For a thorough understanding of the effect of lock-in phenomenon on LCO, a full aeroelastic investigation is required, which models the feedback between the fluid and structural oscillations.

Conclusions

Numerical simulations were conducted to compute the unsteady flowfields around a NACA0012 airfoil that is harmonically oscillating at transonic flow conditions in which large shock oscillations exist. Aerodynamic lift and moment responses to prescribed airfoil-motion excitations revealed that there exists an interaction between the flowfields induced by buffet (shock oscillations even in the absence of airfoil motion) and those induced by airfoil oscillations. At low-amplitude airfoil motions and at frequencies remote from the buffet frequency, the flow exhibits two separate frequencies: that of the buffet and that of the flow response to airfoil oscillation. As the amplitude of airfoil motion increases, the amplitude of the buffet decreases. For airfoil motion at a frequency close to the buffet frequency, the buffet flow response vanishes even for small airfoil-motion amplitudes. There is a broad analogy between the flow physics found in the present study and the flowfield of the von Kármán vortex street found behind a cylinder, with or without the cylinder undergoing a prescribed oscillation [14,15]. In particular, the phenomenon of lock-in is found. A more thorough understanding of the broader implications of the present study for LCO found in certain aircraft awaits a full aeroelastic investigation that models the feedback interaction between fluid and structural oscillations, but it is clear that buffet may play a role in LCO under certain circumstances.

Appendix A: Effect of the Simulation Time Step on Buffet Responses

To study the effect of the simulation time step on buffet responses, simulations were run using computational time steps ranging from 0.00025 to 0.01, where the computational time step $\bar{t}$ is defined as $\bar{t} = ta_\infty/c$. Figure A1 presents time histories of responses to a step angle of attack of 6 deg at Mach 0.72 (set 6 of Table 2). Figure A1 shows that the unsteady response converges with decreasing time step and that a computational time step of 0.0005 or smaller is adequate for these types of analyses.

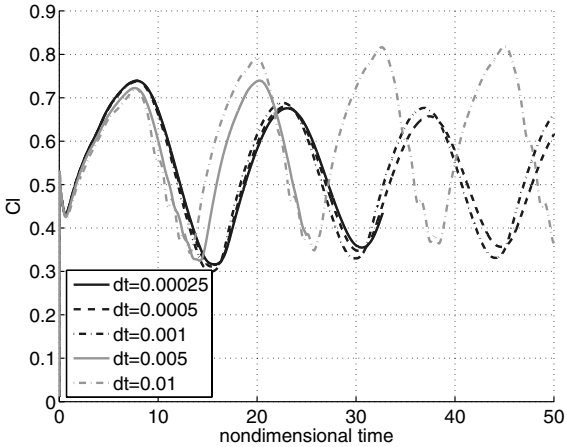

Fig. A1 Unsteady response to a step angle of attack of 6 deg at Mach 0.72, computed with various computational time steps.

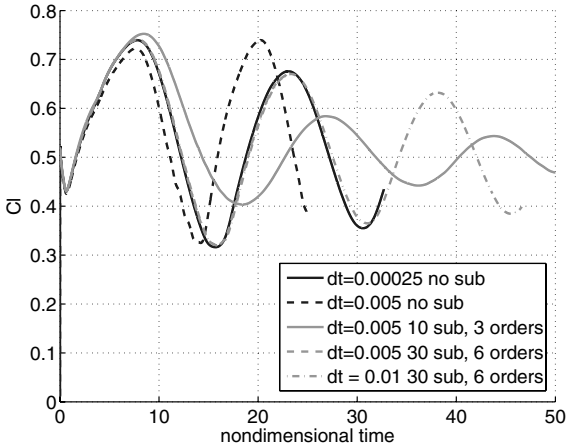

Fig. A2 Unsteady response to a step angle of attack of 6 deg at Mach 0.72, computed with and without dual time steps.

Unsteady analyses were also performed using the code's dual-time-step option. Comparison of simulations performed using dual time steps with those computed without this option but with small time steps is used to ensure that the time integration scheme, which is first-order, indeed yields converged results. In the dual-time-step analyses, a user-defined number of subiterations are computed between two consecutive iterations. A convergence criterion is imposed that terminates the subiteration process following a residual decay of several orders of magnitude defined by the user. Simulations with various parameters (time step, number of subiterations, and termination criterion) revealed that the subiteration process has to be converged to approximately 6 orders of magnitudes to yield realistic results. Figure A2 presents some of the responses computed with dual time steps with various parameters, compared with the analysis without the dual-time-step option. It is seen that by using dual time steps, the CFD simulation can be accurately performed with time steps up to 40 times larger. However, the need to perform 30 subiterations for convergence renders this option computationally expensive and inexpedient. The dual-time-step analyses serve for validation of the accuracy of the simulations without this option, and further analyses are performed without dual time steps, with a small computational time step of 0.0005.

Acknowledgments

I gratefully acknowledge Gil Iosilevskii of the Faculty of Aerospace Engineering, Technion—Israel Institute of Technology, and test pilot Yehuda Shafir, Earl H. Dowell, and Jeffrey P. Thomas of the Department of Mechanical Engineering, Duke University, for their contributions to this study of insight and stimulating suggestions. I am also grateful to Yuval Levy and Yair Moryossef of the Israeli Computational Fluid Dynamics Center for letting me use the Elastic Zonal Navier–Stokes Simulation computational fluid dynamics code and for their support and advice on turbulence models and code validation.

References

[1] Cunningham, A. M., Jr., "The Role of Non-Linear Aerodynamics in Fluid-Structure Interaction," 29th AIAA Fluid Dynamics Conference, AIAA, Washington, D.C., AIAA Paper 98-2423, 1998.

[2] Cunningham, A. M., Jr., and Meijer, J. J., "Semi-Empirical Unsteady Aerodynamics for Modeling Aircraft Limit Cycle Oscillations and Other Non-Linear Aeroelastic Problems," *Proceedings of the International Forum on Aeroelasticity and Structural Dynamics*, Vol. 2, Royal Aeronautical Society, London, June 1995, pp. 74.1–74.14.

[3] Edwards, J. W., Schuster, D. M., Spain, C. V., Keller, D. F., and Moses, R. W., "MAVRIC Flutter Model Transonic Limit Cycle Oscillation Test," NASA TM 210877, 2001.

[4] Edwards, J. W., "Transonic Shock Oscillations and Wing Flutter

Calculated With an Interactive Boundary Layer Coupling Method," 31st AIAA Aerospace Sciences Meeting, AIAA Paper 93-0777, 1993.
[5] Knipfer, A., and Schewe, G., "Investigations of an Oscillating Supercritical 2D Wing Section in a Transonic Flow," 37th AIAA Aerospace Sciences Meeting and Exhibit, AIAA Paper 99-0653, 1999.
[6] Dowell, E. H., and Tang, D., "Nonlinear Aeroelasticity and Unsteady Aerodynamic," *AIAA Journal*, Vol. 40, No. 9, Sept. 2002, pp. 1697–1707.
doi:10.2514/2.1853
[7] Thomas, J. P., Dowell, E. H., and Hall, K. C., "Nonlinear Inviscid Aerodynamic Effects on Transonic Divergence, Flutter, and Limit-Cycle Oscillations," *AIAA Journal*, Vol. 40, No. 4, Apr. 2002, pp. 638–646.
[8] Adar M., Levy, Y., and Gany, A., "Numerical Simulation of Flare Safe Separation," *Journal of Aircraft*, Vol. 43, No. 4, July–Aug. 2006, pp. 1129–1137.
doi:10.2514/1.18033
[9] Barakos, G., and Drikakis, D., "Numerical Simulation of Transonic Buffet Flows Using Various Turbulence Closures," *International Journal of Heat and Fluid Flow*, Vol. 21, 2000, pp. 620–626.
doi:10.1016/S0142-727X(00)00053-9
[10] McDevitt, J. B., and Okuno, A. F., "Static and Dynamic Pressure Measurements on a NACA0012 Airfoil in the Ames High Reynolds Number Facility," NASA TP 2485, 1985.
[11] Wilcox, D. C., "Formulation of the k-ω Turbulence Model Revisited," 45th AIAA Aerospace Sciences Meeting and Exhibit, AIAA Paper 2007-14082007.
[12] Landon, R., "NACA0012 Oscillatory and Transient Pitching in Compendium of Unsteady Aerodynamics Measurements," AGARD TR R-701, Neuilly-sur-Seine, France, 1982.
[13] Relvas, A., and Suleman, A., "Aeroelasticity of Nonlinear Structures Using the Corotational Method," *Journal of Aircraft*, Vol. 43, No. 3, May–June 2006, pp. 749–762.
doi:10.2514/1.15566
[14] Blevins, R. D., *Flow Induced Vibrations*, Van Nostrand Reinhold, New York, 1990.
[15] Dowell, E. H., Hall, K. C., Thomas, J. P., Kielb, R., Spiker, M., Li, A., and Denegri, C. M., Jr., "A New Solution Method for Unsteady Flows Around Oscillating Bluff Bodies," *Proceedings of the IUTAM Symposium on Fluid-Structure Interaction in Ocean Engineering*, Springer–Verlag, New York, 2008.
[16] Young, J., and Lai, J. C. S., "Vortex Lock-In Phenomenon in the Wake of a Plunging Airfoil," *AIAA Journal*, Vol. 45, No. 2, Feb. 2007, pp. 485–490.
doi:10.2514/1.23594

A. Tumin
Associate Editor